ANALYTICAL TREATMENT OF TRANSIENT TEMPERATURE AND THERMAL STRESS DISTRIBUTION IN CW-END-PUMPED LASER ROD
Thermal Response Optimization Study

by

Khalid S. SHIBIB*, Mayada M. TAHER, and Mohammad A. MAHDI
Department of Laser and Optoelectronics Engineering, University of Technology, Baghdad, Iraq

Original scientific paper
DOI: 10.2298/TSCI110701137S

The analytical solution of transient temperature distribution and Tresca failure stress in cw-end-pumped laser rod has been derived using integral transform method. The analytical result is compared with numerical solutions presented by other works and good agreement has been found. Analytical solution with its clear physical meaning and its explicit form permits to predict the influence of various factors on the solution. The optical path difference which gives a valuable means to quantify the optical properties of laser material such as designed beam quality, will converge to a constant value as steady-state temperature distribution is reached. One can obtain the dominate factors which affect the laser response to bring the laser rod to the thermal equilibrium; it has been found that fast response can be achieved by reducing pumping power, increasing extracted heat from the rod, choosing a crystal having high thermal diffusivity and decreasing laser rod radius while its volume remains constant. One final advantage of the analytical solution is that a fast result can be obtained where the numerical solution usually is a time consuming technique.

Key words: *integral transform method, heat transfer, laser rod, Tresca failure criteria, optical path difference, response optimization*

Introduction

In spite of various laser types exist; diode-end-pumped solid-state laser has drawn much attention due to its several advantages: it has higher efficiency than lamp-pumped laser, increasing peak power due to the long upper state lifetimes, a simpler cooling geometry, and high beam quality [1], besides the design of these systems suffer from the limitation of dissipated heat that affect the operation of the system. It may lead to changes in the refractive index, degradation of laser characteristics, strain, and even to destruction of active media [2].

Many laser applications required fast laser system response (*i. e*. reaching a quickly steady-state situation to obtain designed beam quality and operation conditions). This required knowledge in transient thermal behavior of laser rod and the time on which steady-state operation can be reached to provide designed beam quality, which has important feathers in many laser applications such as measurements, welding process, control systems and military applications.

* Corresponding author; e-mail: assprofkh@yahoo.com

With the availability of commercial packages, a detailed study of such a problem is available. These packages severe from the lack of validation require long exercising and are time consuming. A new direction in this field is solving analytically the partial differential equations. These solutions have clear physical concepts, logical reasoning, and they are usually expressed in an explicit function form that can indicate the influence of various factors. So they are still widely used up to date [3-6].

Here in order to investigate the temperature distribution, the thermally induced stresses and the thermal response, an analytical thermal model of the laser gain medium that determining the transient temperature and the corresponding induced maximum stresses on an isotropic laser rod, is derived using the integral transform method. The model has been verified through a commercial ABAQUS package [7] done by [5], and the model has been applied to cw pumped laser rods starting from the rest and a good agreement has been found between the results. The time required to reach the steady-state operation condition is obtained analytically also the steady-state solution for temperature and maximum stress is obtained. The work has been extended to predict the temperature distribution and the maximum stress after switching off the pumping power until the laser rod is brought again to rest, also the influence of various factors that affect the fast response of the laser beam are studied.

Theory

Thermal analyses

The prediction of the temperature distribution inside the laser rod is a first step for determining the influence of the thermal effects on the laser performance. The part of absorbed power that converts to heat act as a heat source and must be dissipated efficiently to maintain good system operation. For circular symmetry, the transient temperature distribution through laser rod can be written as [8]:

$$\frac{\partial^2 T}{\partial r^2}+\frac{1}{r}\frac{\partial T}{\partial r}+\frac{\partial^2 T}{\partial z^2}+\frac{Q}{k}=\frac{\rho c}{k}\frac{\partial T}{\partial t} \tag{1}$$

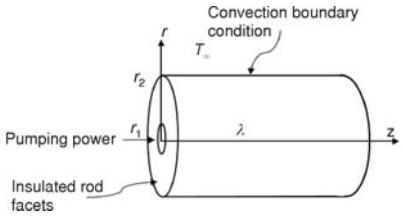

Figure 1. Studied domain and boundary conditions of laser rod

The boundary conditions are, see fig. 1:

$$T = T_\infty \quad \text{at} \quad t = 0 \tag{1a}$$

$$k\frac{\partial T}{\partial r} = h(T_\infty - T) \quad \text{at} \quad r = r_2 \tag{1b}$$

$$\frac{\partial T}{\partial z} = 0 \quad \text{at} \quad z = 0, \quad z = \lambda \tag{1c}$$

$$\frac{\partial T}{\partial r} = 0 \quad \text{at} \quad r = 0 \tag{1d}$$

The initial and environmental temperatures equal to 25 °C. The heat generation from absorbed power can be written as [9]:

$$Q = \begin{cases} \dfrac{\eta\alpha P_{ab}\exp(-\alpha z)}{\pi r_1^2[1-\exp(-\alpha\ell)]} & 0 \le r \le r_1,\ t \ge 0 \\ 0 & r_1 \le r \le r_2,\ t \ge 0 \\ 0 & t < 0 \end{cases} \tag{2}$$

The standard solution for eq. (1) is [8]:

$$\theta = \sum_{m=1}^{\infty}\sum_{p=1}^{\infty}\frac{R_0(\beta_m, r)Z(\eta_p, z)}{N(\beta_m)N(\eta_p)}\exp\left[-\frac{k}{\rho c}(\beta_m^2+\eta_p^2)t\right]\cdot \cdot\left\{\frac{1}{\rho c}\int_{t'=0}^{t}\exp\left[\frac{k}{\rho c}(\beta_m^2+\eta_p^2)t'\right]\ddot{\bar{g}}(\beta_m,\eta_p,t')\,\mathrm{d}t'\right\} \tag{3}$$

where

$$\ddot{\bar{g}}(\beta_m,\eta_p,t') = \int_{z=0}^{\lambda}\int_{r=0}^{r_1} r'R_0(\beta_m,r')Z(\eta_p,z')g(t')\,\mathrm{d}r'\mathrm{d}z' \tag{3a}$$

also
$$R_0(\beta_m, r) = J_0(\beta_m r) \tag{3b}$$

$$\frac{1}{N(\beta_m)} = \frac{1}{N_m} = \frac{2k^2\beta_m^2}{r_2^2 J_0(\beta_m r_2)(h^2+k^2\beta_m^2)} \tag{3c}$$

$$Z(\eta_p, z) = \cos(\eta_p z) \tag{3d}$$

By using convection boundary condition, the roots can be obtained from:

$$hJ_0(b_m r_2) - k\beta_m J_1(\beta_m r_2) = 0 \tag{4a}$$

Also for insulated rod facets:
$$\frac{1}{N(\eta_p)} = \frac{1}{N_p}\begin{bmatrix}\frac{2}{\lambda}\ \text{for}\ \eta_p \neq 0\\ \frac{1}{\lambda}\ \text{for}\ \eta_p = 0\end{bmatrix} \tag{4b}$$

where its root η_p is obtained from:

$$\sin(\eta_p\lambda) = 0 \tag{4c}$$

The roots included $\eta_p = 0$ (*i. e*. Insulated boundary at the facets of the rod).

Then eq. (3) can be written as:

$$\theta = T - T_\infty = \sum_{m=1}^{\infty}\frac{J_0(\beta_m r)}{\rho c N_m \lambda}\exp\left(-\frac{k}{\rho c}\beta_m^2 t\right)\left[\int_{\tau=0}^{\tau}\exp\left(\frac{k}{\rho c}\beta_m^2\tau\right)g_m(\tau)\mathrm{d}\tau\right] + + \sum_{m=1}^{\infty}\sum_{p=1}^{\infty}\frac{2J_0(\beta_m r)\cos(\eta_p z)}{\rho c N_m \lambda}\exp\left[-\frac{k}{\rho c}(\beta_m^2+\eta_p^2)t\right]\left\{\int_{\tau=0}^{\tau}\exp\left[\frac{k}{\rho c}(\beta_m^2+\eta_p^2)\tau\right]g_{mp}(\tau)\mathrm{d}\tau\right\} \tag{5}$$

where

$$g_m(\tau) = \int_0^{\lambda}\int_0^{r_1}\frac{\eta\alpha P_{ab}}{\pi r_1^2 k}\exp(-\alpha z)J_0(\beta_m r)r\,\mathrm{d}r\mathrm{d}z \tag{5a}$$

$$g_{mp}(\tau) = \int_0^{\lambda}\int_0^{r_1}\frac{\eta\alpha P_{ab}}{\pi r_1^2 k}J_0(\beta_m r)\exp(-\alpha z)\cos(\eta_m z)r\,\mathrm{d}r\mathrm{d}z \tag{5b}$$

Assuming cw mode then at a time less than or equal to the time necessary to reach the steady-state operation condition, the transform of time (τ) is equal to t in eq. (5). The transient solution can be obtained starting from the rest and the time necessary to reach steady-state operation condition can be obtained as the difference in temperatures for certain location between two subsequent time steps is dimensioned. For the solution above, the temperature history in laser rod can be obtained until the steady-state condition is reached. A further simplifying can be achieved by carrying the time integration and integration of $g_m(\tau)$ and $g_{mp}(\tau)$ then for $t \leq t_s$:

$$\theta = T - T_\infty = \sum_{m=1}^{\infty} \frac{\eta P_{ab} J_0(\beta_m r) J_1(\beta_m r_1)}{\pi r_1 k N_m \lambda \beta_m^3} \left[1 - \exp\left(-\frac{k}{\rho c} \beta_m^2 t \right) \right] + \\ + \sum_{m=1}^{\infty} \sum_{p=1}^{\infty} \frac{2\eta\alpha^2 P_{ab} J_1(\beta_m r_1) J_0(\beta_m r) \cos(\eta_p z)[1 - \cos(\eta_p \lambda)\exp(-\alpha\lambda)]}{\pi r_1 \beta k N_m \lambda (\beta_m^2 + \eta_p^2)(\alpha^2 + \eta_p^2)[1 - \exp(-\alpha\lambda)]} \cdot \\ \cdot \left[1 - \exp\left(-\frac{k}{\rho c} (\beta_m^2 + \eta_p^2) t \right) \right] \tag{6}$$

For time $t > t_s$, incorporating time integration in eq. (5) with limits of time integration from t_s to t then:

$$\theta = T - T_\infty = \sum_{m=1}^{\infty} \frac{\eta P_{ab} J_0(\beta_m r) J_1(\beta_m r_1)}{\pi r_1 k N_m \lambda \beta_m^3} \left\{ \exp\left[\frac{k}{\rho c} \beta_m^2 (t - t_s) \right] - \exp\left(-\frac{k}{\rho c} \beta_m^2 t \right) \right\} + \\ + \sum_{m=1}^{\infty} \sum_{p=1}^{\infty} \frac{2\eta\alpha^2 P_{ab} J_1(\beta_m r_1) J_0(\beta_m r) \cos(\eta_p z)[1 - \cos(\eta_p \ell)\exp(-\alpha\ell)]}{\pi r_1 \beta_m k N_m \ell (\beta_m^2 + \eta_p^2)(\alpha^2 + \eta_p^2)[1 - \exp(-\alpha\ell)]} \cdot \\ \cdot \left\{ \exp\left[\frac{k}{\rho c} (\beta_m^2 + \eta_p^2)(t - t_s) \right] - \exp\left[-\frac{k}{\rho c} (\beta_m^2 + \eta_p^2) t \right] \right\} \tag{7}$$

The steady-state solution can be also obtained by setting the time equal to infinity where the term that contains time in eq. (6) is vanished then the solution for the temperature in the thermal equilibrium can be written as:

$$\theta = T - T_\infty = \sum_{m=1}^{\infty} \frac{\eta P_{ab} J_0(\beta_m r) J_1(\beta_m r_1)}{\pi r_1 k N_m \lambda \beta_m^3} + \\ + \sum_{m=1}^{\infty} \sum_{p=1}^{\infty} \frac{2\eta\alpha^2 P_{ab} J_1(\beta_m r_1) J_0(\beta_m r) \cos(\eta_p z)[1 - \cos(\eta_p \lambda)\exp(-\alpha\lambda)]}{\pi r_1 \beta_m k N_m \lambda (\beta_m^2 + \eta_p^2)(\alpha^2 + \eta_p^2)[1 - \exp(-\alpha\lambda)]} \tag{8}$$

In cw mode operation, it is important to reach the steady-state condition where the temperature and the designed performance such as beam quality which depend on the optical path difference (OPD) can be reached its designed value, this situation can provide designed beam quality since the optical path difference will reach a constant value as the steady-state temperature distribution is reached, which has important feathers in many laser applications such as measurements, welding process, control system and many military applications. Equation (8) stands for this case where a comparison between the transient and steady-state temperatures is made and as the transient temperature reaching 99.9% from the steady-state temperature every where in the laser rod, it can be regarded as a steady-state condition.

Stress analysis

Following the work of Bernhardi [5], LASCAD package [10], making use of a plain-strain approximation (*i. e.* $\lambda / r_2 \gg 1$), neglecting the axial stress and assuming the radial and hoop stresses can be written as:

$$\sigma_r = \frac{\gamma E}{1 - \nu} \left(\frac{1}{r_2^2} \int_0^{r_2} \theta r \mathrm{d}r - \frac{1}{r^2} \int_0^{r} \theta r \mathrm{d}r \right) \tag{9}$$

$$\sigma_\theta = \frac{\gamma E}{1 - \nu} \left(\frac{1}{r_2^2} \int_0^{r_2} \theta r \mathrm{d}r + \frac{1}{r^2} \int_0^{r} \theta r \mathrm{d}r - \theta \right) \tag{10}$$

Then the maximum shear stress is used to predict failure which is known as Tresca failure criterion and for plain strain approximation it can be written as [1, 5, 10, 11]:

$$\sigma_T = |\sigma_\theta - \sigma_r| = \frac{\gamma E}{1-\nu}\left|\frac{2}{r^2}\int_0^r \theta r \mathrm{d}r - \theta\right| \tag{11}$$

Incorporating $z = 0$ in eqs. (6) and (7), carrying the integration and knowing that $J_2(x) = 2J_1(x)/x - J_0(x)$, then the Tresca stress history for $t \le t_s$ can be written as:

$$\sigma_T = \frac{\gamma E}{(1-\nu)}\left|\sum_{m=1}^{\infty}\frac{\eta P_{ab} J_2(\beta_m r) J_1(\beta_m r_1)}{\pi r_1 k N_m \lambda \beta_m^3}\left[1-\exp\left(-\frac{k}{\rho c}\beta_m^2 t\right)\right] + \right.$$
$$\left. + \sum_{m=1}^{\infty}\sum_{p=1}^{\infty}\frac{2\eta\alpha^2 P_{ab} J_1(\beta_m r_1) J_2(\beta_m r)[1-\cos(\eta_p \ell)\exp(-\alpha\ell)]}{\pi r_1 \beta_m k N_m \lambda(\beta_m^2+\eta_p^2)(\alpha^2+\eta_p^2)[1-\exp(-\alpha\ell)]}\left\{1-\exp\left[-\frac{k}{\rho c}(\beta_m^2+\eta_p^2)t\right]\right\}\right| \tag{12}$$

The stress history for $t > t_s$ can be written as:

$$\sigma_T = \frac{\gamma E}{(1-\nu)}\left|\sum_{m=1}^{\infty}\frac{\eta P_{ab} J_2(\beta_m r) J_1(\beta_m r_1)}{\pi r_1 k N_m \ell \beta_m^3}\left\{\exp\left[\frac{k}{\rho c}\beta_m^2(t-t_s)\right]-\exp\left(-\frac{k}{\rho c}\beta_m^2 t\right)\right\} + \right.$$
$$+\sum_{m=1}^{\infty}\sum_{p=1}^{\infty}\frac{2\eta\alpha^2 P_{ab} J_1(\beta_m r_1) J_2(\beta_m r)[1-\cos(\eta_p \ell)\exp(-\alpha\ell)]}{\pi r_1 \beta_m k N_m \ell(\beta_m^2+\eta_p^2)(\alpha^2+\eta_p^2)[1-\exp(-\alpha\ell)]}\cdot$$
$$\left.\cdot\left\{\exp\left[\frac{k}{\rho c}(\beta_m^2+\eta_p^2)(t-t_s)\right]-\exp\left[-\frac{k}{\rho c}(\beta_m^2+\eta_p^2)t\right]\right\}\right| \tag{13}$$

By using eqs. (11) and (8), the steady-state Tresca stress can be written as:

$$\sigma_T = \frac{\gamma E}{1-\nu}\left|\sum_{m=1}^{\infty}\frac{\eta P_{ab} J_2(\beta_m r) J_1(\beta_m r_1)}{\pi r_1 k N_m \lambda \beta_m^3} + \right.$$
$$\left. + \sum_{m=1}^{\infty}\sum_{p=1}^{\infty}\frac{2\eta\alpha^2 P_{ab} J_1(\beta_m r_1) J_2(\beta_m r)[1-\cos(\eta_p \lambda)\exp(-\alpha\lambda)]}{\pi r_1 \beta_m k N_m \lambda(\beta_m^2+\eta_p^2)(\alpha^2+\eta_p^2)[1-\exp(-\alpha\lambda)]}\right| \tag{14}$$

Validation

Although the analytical treatment of the thermal problem has many limitations in dealing with non-uniform shapes, the temperature dependent physical properties, and the boundary conditions, it is of interest to compare their result by the numerical result of a same physical domain and boundary conditions [12]. Reported results given by [5] are used to verify the analytical solution of cw pumped, 4% doped, Tm:YLF laser rod with λ = 12 mm, r_2 =1.5 mm. The pumped beam was a near top-hat profile and pumped radius of $r_1 = 470$ μm is in the middle of the crystal, the convection heat transfer coefficient is assumed to be 0.9 Wcm^2/K, the thermal and optical properties of Tm:YLF crystal are taken from [5]. Using a pumping power of 47.2 W the above condition will cause failure as predicted by [13], where the maximum Tresca stress was 33-40 MPa. Note that this boundary conditions will be referred as normal in the subsequent discussion. The result of this work predicts that this power for the same rod can reach a maximum Tresca stress of 41.9 MPa as the solution reaches the steady-state condition, fig. 2(a), which in-

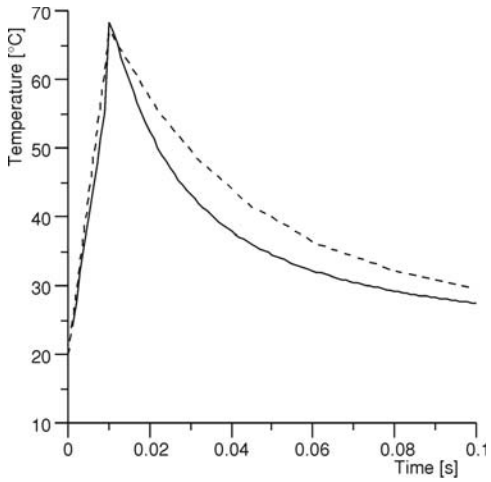

Figure 2(a). The stress and the temperature history in Tm:YLF laser rod, the solid line indicates the maximum stress history and dashed line indicates the corresponding temperature

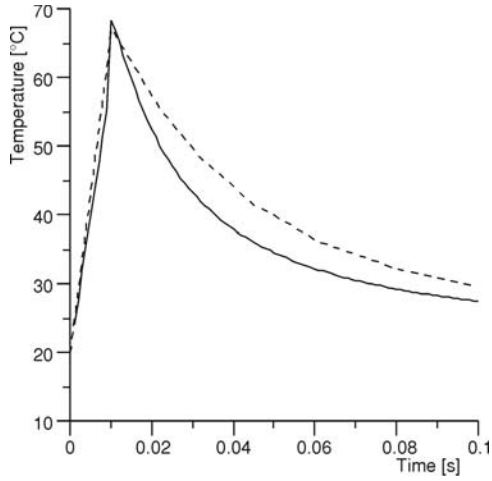

Figure 2(b). The analytically (solid line) and the numerically (dashed line) predicted temperature in the center of the Tm:YLF rod as function of time at 200 W pumping power for the first 10 ms and a cut-off time for 90 ms; both solutions have an average heat factor of 0.33 [5]

dicates the history of Tresca stress and the temperature history of the same position. This value is also obtained by reference [5], where the finite element solution using ABAQUS packages predict that the maximum Tresca stress of 41 MPa for the same laser rod and boundary conditions.

An additional comparison has been made between the analytical temperature history at the center of the cw-end-pumped of the Tm:YLF laser rod and that obtained numerically by reference [5], assuming that both have the aforementioned normal boundary conditions and a good agreement has been found which may also verify the analytical solution of this work, fig. 2(b).

Results and discussion

The analytical solution of the transient axis-symmetry temperature distribution and the maximum thermal stress in the cw-end-pumped laser rod is derived using integral transform method; different types of boundary conditions including the effect of the cw-end-pumping power have been studied. The obtained result has been compared with the finite element solution of such problems and a good agreement has been found.

By establishing the analytical solution for the temperature distribution and the subsequent thermal stress in the laser rod, the expected absorbed power level that could cause rod failure due to the stress concentration is also obtained. The history of the temperature and the thermal stress for the domain is predicted. Different thermal boundary conditions can be imposed [8], to deal with the realistic boundary conditions that the laser rod is subjected to. Insulated facets are assumed through the solution eqs. 4(b) and (c) and it is just an approximation where the real condition is that the facets are subjected to convection boundary condition. This may complicate and vary the final form of the analytical solution. But still the result is of a good near by even with this assumption as tested by the authors.

A program has been written in the Visual basic 6 to obtain the roots β_m, η_p, and the values of N_m and N_p, which are used to predict the temperature distribution by using eqs. (6)-(8).

Using Tresca failure criterion, eqs. (12)-(14) are used to estimate the maximum induced stress in the laser rod. Steady-state temperature distribution and Tresca failure criterion are, firstly obtained and as the transient solution for the temperature reaching 99.9% from the steady-state temperature then one can say that the thermal equilibrium has been reached. The transient solution can be extended to the period when the pumping is switched off and the time required to bring the rod back to rest can be also obtained.

The transient temperature distribution towards the steady-state has been predicted and the time required to reach the thermal equilibrium is also obtained. It is well known that the beam quality that depends mainly on the optical path difference can be affected by the transient temperature distribution, since it depends mainly on the temperature distribution through the laser rod and its effects [13], so it is of importance to know how much it takes to reach the steady-state temperature distribution which leads to stabilize optical path difference.

The solution has been tested to predict at which the time the thermal equilibrium can be achieved at different absorbed powers, fig. 3. Equation 8, clearly shows that the maximum temperature is occurred at the center of the pumped end (*i. e*. $J_0(\beta_m r) = 1$), since the Bessel function reaches its maximum value when radius is equal to zero. It is found that the temperature at the center of the rod takes the longest time to reach the steady-state, so that it has been chosen to see whether the system is reached this situation or not. The maximum temperature history (at the center of near pumped face) for the Tm:YLF laser rod having the aforementioned normal boundary conditions are tested at different power levels, fig. 3. It can bee seen that as the absorbed power increases for a certain rod and boundary conditions, then more time is required to reach the steady-state condition, due to the increasing of induced heat, while its dissipation is held approximately constant.

From eqs. (6)-(8), it is clear that for the aforementioned rod, doubling the convection heat transfer coefficient will reduce the time necessary to reach the thermal equilibrium, where the time required to reach this condition will be reduced from 5.2 s to 3.6 s, fig. 4. This reduction in time is also observed after the pumping power is switched off. It is also ob-

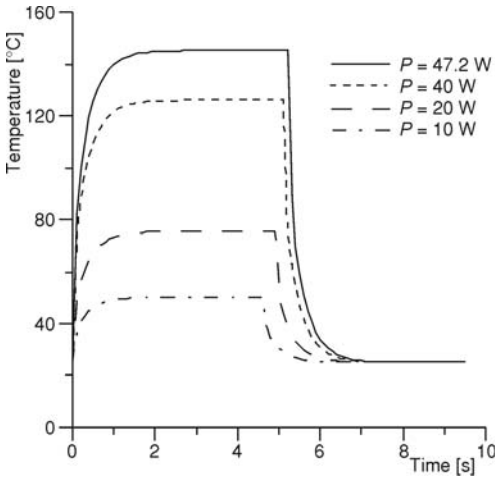

Figure 3. The history of the maximum temperature for the different levels of absorbed power in Tm:YLF laser rod

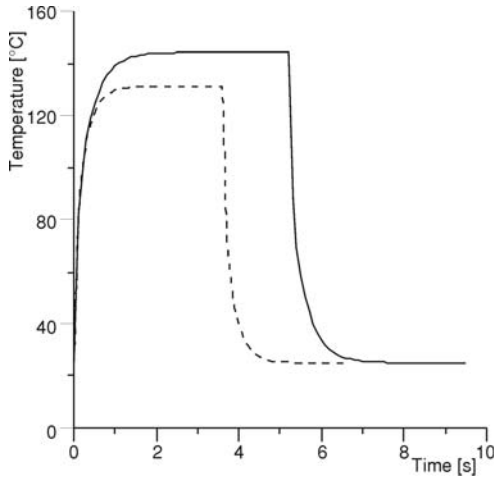

Figure 4. The maximum temperature history for Tm:YLF laser rod at different heat transfer coefficients; solid line for h = 0.9/cm^{2}K and for dashed line h is doubled

served that the maximum temperature in the laser rod is reduced. All these observations can be explained by the fact that more heat will flow out of the laser rod as the convection heat transfer coefficient is increased.

Considering other parameters in eqs. (6) and (7), it well known that the larger the value of thermal diffusivity, the faster heat will diffuse through the material [14], which means that increasing the thermal diffusivity (D) will lead to reduce the time necessary for reaching the steady-state condition, this can be achieved by either increasing the thermal conductivity or decreasing the product of ρc, both factors will reduce the time necessary to reach the thermal equilibrium.

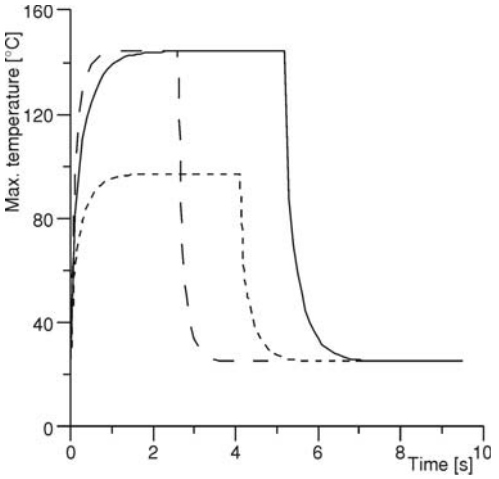

Figure 5. The maximum temperature history at the different thermal diffusivity; solid line for Tm:YLF rod, short-dashed line for doubling the thermal conductivity, long-dashed line for halving the thermal specific heat

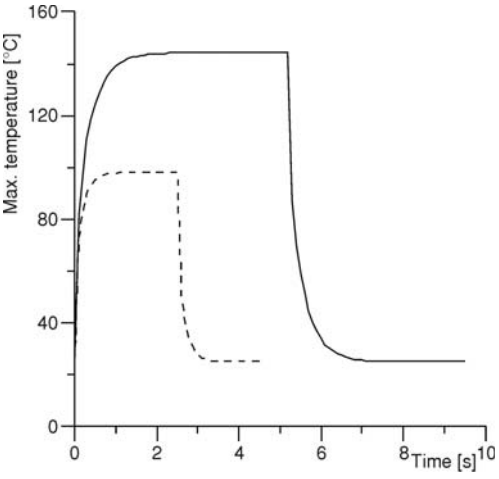

Figure 6. The combined effects of various factors on the temperature history of the laser rod; solid line for Tm:YAF, dashed line for Nd:YAG

Without refereeing to a special material as the thermal diffusivity is increased, a significant reduction in the two periods (reaching a steady-state operation condition and bring to rest) is observed, fig. 5. Some significant observations can be obtained from the analytical solution which is indicated in fig. 5; it is that the decreasing in the value of the product ρc is more effective than the increasing in the thermal conductivity if one intends to decrease the response time.

One can conclude that when there is a choice in selecting a material of the laser rod, it seems that Nd:YAG (which has a higher thermal diffusivity than other types of crystals usually used in cw-end-pumped method) is very convenient to be used as a crystal in laser system to achieve fast response (*i. e.* reaching the steady-state operation or bringing to rest rapidly).

Now all these factors are incorporated together to see their combined effects on the temperature history of the laser rod; the crystal is changed to Nd:YAG , the power is halved, the heat transfer coefficient is doubled, a significant reduction is observed in the time required to reach the steady-state operation condition and the time required to bring the rod to rest again, fig. 6. It takes 2.5 s to reach the steady-state condition while this period for Tm:YLF is 5.2 s.

An interesting finding from the analytical solution is that for the same volume of the laser rod as the radius decreases (*i. e.* lengthen the rod), then a significant reduction in the re-

sponse time is observed, see fig. 7. This is due to the fact that the agent of cooling will be more effective, since more surface area is subjected to convection heat transfer and as the heat is assumed to generate steadily through the rod, then the rod will be brought quickly to the thermal equilibrium.

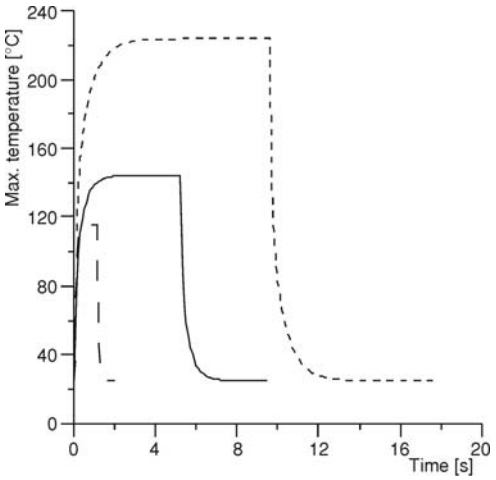

Figure 7. The maximum temperature history for different rod and pumping geometry; long-dashed line for halving radius, short-dashed line for multiplying the radius by 1.5, assuming a constant laser rod volume

Conclusions

The analytical solution of the transient temperature and the Tresca failure stress on an end pumped laser rod is derived using integral transform method. The result is compared to numerical solutions, and good agreement has been found. The history of the temperature and the Tresca failure stress criterion has been obtained for the laser rod starting from the rest until it reaches the steady-state condition. The solution is extended to the time when pumping is switching off until the rod is brought to the rest again. It found that the factors which reduce the time required to achieve the thermal equilibrium (*i. e.* steady-state operation condition and brought to rest again) are:

- increasing the convection heat transfer coefficient,
- decreasing the power level, and
- choosing a crystal of high thermal diffusivity (decreasing in the product of is more effective than increasing the thermal conductivity).
- decreasing the radius of the laser rod while its volume remains constant.

The analytical solution permits quick prediction of the effect of the above mentioned parameters on the temperature and the stress history and also can guide a designer on which type of laser rod and boundary conditions could quickly establish the thermal equilibrium.

Nomenclatures

c – specific heat [Jkg^{-1}K^{-1}]
D – thermal diffusivity (= $k/\rho c$), [m^{2}s^{-1}]
E – Young modulus of elasticity, [MPa]
h – convection heat transfer coefficient, [Wm^{-2}K^{-1}]
k – thermal conductivity, [Wm^{-1}K^{-1}]
p – power, [W]
r – radial co-ordinates, [m]
Q – heat generation, [Wm^{-3}]
T – temperature, [°C]
t – time, [s]
z – longitudinal co-ordinate, [m]

Greek symbols

α – absorption coefficient, [m^{-1}]
β_m, η_p – roots of equations
γ – linear expansion coefficient, [K^{-1}]
η – heat factor, [–]
θ – temperature difference, [°C]
λ – laser rod length, [m]
ρ – density, [kgm^{-3}]
σ – thermal stress, [MPa]
τ – transformation time, [s]
υ – Poisson ratio, [–]

Subscript or superscript

ab – absorb
c – center
e – edge
r – radial
s – steady-state
T – Tresca

q – hoop
∞ – environmental
' – transformed co-ordinate or time
1 – pumping
2 – outside

References

[1] Bernhardi, E. H., Modeling Diode-Pumped Solid-State Lasers, M. Sc. thesis, School of Physics, University of KwaZulu-Natal, Durban, South Africa, 2008
[2] Mukhin, I., *et al*., Reduction of Thermally Induced Depolarization of Laser Radiation in [110] Oriented Cubic Crystals, *Optics Express, 17* (2009), 7, pp. 5496-5501
[3] Huang, F., *et al*., Modeling and Resolving Calculation of Thermal Effect in Face-Pumped High Power Heat Capacity Disk Laser, *Proc. of SPIE, 6823* (2007), 11, pp. 1-8
[4] Usievich, B. A., *et al*., Analytical Treatment of Thermal Problem in Axially Pumped Solid State Lasers, *IEEE J. of Quantum Electronics, 37* (2001), 9, pp. 1210-1214
[5] Bernhardi1, E. H., *et al*., Estimation of Thermal Fracture Limits in Quasi-Continuous-Wave end-Pumped Lasers through a Time-Dependent Analytical Model, *Optics Express, 16* (2008), 15, pp.11115-11123
[6] Li, Z., *et al*., A Study of the Axisymmetric Thermal Strain in a Laser Rod with Longitudinal Temperature Rise, *Applied Thermal Engineering, 29* (2009), 14-15, pp. 2927-2934
[7] ***, *ABAQUS Finite Element Software Package*, 2008 http://www.simulia.com/products/abaqus_fea.html
[8] Ozisik, M. N., *Heat Conduction*, John Wiley and Sons, New York, USA,1980, pp. 543-544
[9] Cousins, A. K., Temperature and Thermal Stress Scaling in Finite-Length End-Pumped Laser Rods, *IEEE Journal of Quantum Electronics, 28* (1992), 4, pp.1057-1069
[10] ***, *LASCAD Manual*, 2008, https://www.las-cad.com/files/PP_FEA.pdf.
[11] Tian, Y., *et al*.,Time-Dependent Analytical Model of Thermal Effects in Continuous-Wave end-Pumped Tm:Yap Lasers, *Applied Phys B, 103* (2011), pp. 107-112
[12] Shibib, K. S., *et al*., Thermal and Stress Analysis in Nd:YAG Laser Rod with Different Double end Pumping Method, *Thermal Science, 15* (2011), Suppl. 2, pp. S399-S407
[13] Koechner, W., *Solid-State Laser Engineering*, 6th ed., Springer Series .in Opt. Sci., USA, 2006
[14] Holman, J. P., *Heat Transfer in SI Units*, 5th ed., McGraw-Hill International Book Company, Japan, 1981, p. 5

Paper submitted: July 1, 2011
Paper revised: December 1, 2011
Paper accepted: December 19, 2011